

## Thermal properties in cured natural rubber/styrene butadiene rubber blends

S. Goyanes<sup>a,b</sup>, C.C. Lopez<sup>a,1</sup>, G.H. Rubiolo<sup>a,b,c</sup>, F. Quasso<sup>d</sup>, A.J. Marzocca<sup>a,\*</sup>

<sup>a</sup> Universidad de Buenos Aires, Facultad de Ciencias Exactas y Naturales, Dto. de Física,

Lab. Propiedades Mecánicas de Polímeros y Materiales Compuestos, Ciudad Universitaria, Pabellón 1, 1428 Buenos Aires, Argentina

<sup>b</sup> Consejo Nacional de Investigaciones Científicas y Técnicas (CONICET), Argentina

<sup>c</sup> Departamento de Materiales, CNEA, Av. del Libertador 8250, 1424 Buenos Aires, Argentina

<sup>d</sup> Dipartimento di Fisica, Politecnico di Milano, Piazza Leonardo da Vinci 32, I-20133 Milano, Italy

Received 3 August 2007; received in revised form 17 January 2008; accepted 17 February 2008

Available online 23 February 2008

### Abstract

Blends of natural rubber (NR) and styrene butadiene rubber (SBR) were prepared with sulfur and *n*-*t*-butyl-2-benzothiazole sulfonamide (TBBS) as accelerator, varying the amount of each polymer in the blend. Samples were analysed by rheometer curing at 433 K until their maximum torque was reached. The miscibility among the constituent polymers of the cured compounds was studied in a broad range of temperatures by means of differential scanning calorimetry, analyzing the glass transition temperatures of the samples. The specific heat capacity of the compounds was also determined. Thermal diffusivity of the samples was measured in the temperature range from 130 to 400 K with a new device that performs measurements in vacuum. The thermal results are explained on the basis of the structure formed during the vulcanization of the samples considering the variation of the crosslink density of each phase. Finally, a serial thermal conduction model that takes into account the contribution of each phase to the thermal diffusivity was used to fit the experimental results. © 2008 Elsevier Ltd. All rights reserved.

**Keywords:** NR/SBR blends; Thermal diffusivity; Glass transition temperature; Specific heat; Vulcanization

### 1. Introduction

Values of thermal diffusivity  $\alpha$  and thermal conductivity  $k$  are needed for heat flow calculations, and for the determination of structure-properties

relationships and materials selection and comparison.

Thermal diffusivity is one of the less studied thermal properties of materials. This can be attributed in part to the fact that there are not many commercial devices to measure this physical property.

Several devices for measuring thermal diffusivity were reported in literature [1–6]. An important limitation of these devices is that they cannot work below room temperature or can only be used for very small samples. This fact becomes a problem in the case of filled polymers.

\* Corresponding author. Fax: +54 11 45763357.

E-mail address: [marzo@df.uba.ar](mailto:marzo@df.uba.ar) (A.J. Marzocca).

<sup>1</sup> Present address: Department of Nuclear Science and Engineering, Massachusetts Institute of Technology, Cambridge, MA 02139, USA.

The measurement of the thermal diffusivity of low thermal conduction materials is based on the determination time dependence of temperature in a specific location of the sample as consequence of known thermal boundary conditions.

In our research group we have presented an improved method for the determination of thermal diffusivity of elastomeric compounds [7–10]. By using this method, the thermal diffusivity is estimated through the glass transition range [8].

An interesting area of study is the thermal diffusivity of cured elastomer blends. There are two main reasons for blending elastomers: the first is the combination of properties of each of the polymer in the blend and the second is to obtain a new compound that improves specific properties with respect to the constituent polymers. In fact, rubber blending is one of the most effective methods to produce new compounds for specific requirements.

The physical properties of immiscible two-phase blends depend on the properties of each constituent phase: the morphology, dispersion and stiffness of each phase play a significant role in the final properties of the blend.

Elastomer blends find widespread use in several technological applications. Typical compounds include natural rubber (NR), polybutadiene rubber (BR) and styrene-butadiene rubber (SBR) blends. In this case the phase behavior is very complicated because macro and micro phase separation can take place [11]. The classical case of immiscibility is marked by the appearance of two unbroadened glass transition temperatures ( $T_g$ ) which are unchanged from that of the component (non-blended) polymers. Also, it is important to know that any shift of  $T_g$  could indicate partial solubility [12]. In cases of partial miscibility blends, two glass transitions may be detected at temperatures that are different from the corresponding glass transition temperatures of the components. In such cases, the  $T_g$  of the polymer with the lowest glass transition temperature increases and, conversely, the  $T_g$  of the polymer with the highest glass transition temperature decreases, thus shortening the temperature interval between the two glass transitions. The extent of this shortening is a measure of miscibility and, in the ideal case of a miscible blend there is a single  $T_g$ .

Saxena et al. [13] studied and measured the thermal conductivity of cured SBR with particles of NR latex waste as filler, in a temperature range of 100–300 K. They reported a broad peak in the thermal

conductivity in the glass transition region of the compounds.

In this work we introduce a new device used to estimate the thermal diffusivity in cured natural rubber (NR)/styrene butadiene rubber (SBR) blends. These measurements are complemented with specific heat capacity measurements performed with DSC. The thermal properties are analyzed considering the structure obtained in the elastomer phases during vulcanization.

## 2. General theory

Knowledge of the thermal behavior of a sample is an important requirement in the design of the material. Considering an isotropic material of density  $\rho$ , specific heat capacity  $c_p$  and thermal conductivity  $k$ , the general differential equation for transient conduction of heat is defined as

$$\rho c_p \frac{\partial \theta}{\partial t} = \nabla \cdot (k \nabla \theta) + \frac{dQ}{dt} \quad (1)$$

This equation must be solved in order to obtain the temperature  $\theta$  at any time taking into account the geometry and the boundary conditions of the sample. In Eq. (1)  $Q$  is an internal heat source that may be due to a chemical reaction of the material. Knowledge of the thermal parameters,  $k$ ,  $c_p$  and  $Q$  are essential to accurately predict the behavior of the material under different heating conditions.

In the case of materials where no internal heat source is present ( $dQ/dt = 0$ ), Eq. (1) can be rewritten in the one-dimensional case as

$$\frac{\partial}{\partial x} \left( k \frac{\partial \theta}{\partial x} \right) = \rho c_p \frac{\partial \theta}{\partial t} \quad (2)$$

$$\frac{\partial^2 \theta}{\partial x^2} + \frac{1}{k} \frac{\partial k}{\partial x} \frac{\partial \theta}{\partial x} = \frac{1}{\alpha} \frac{\partial \theta}{\partial t} \quad (3)$$

where  $\alpha = k/c_p\rho$  is the thermal diffusivity of the material. This parameter relates energy flux to energy gradient.

The reduction of Eq. (3) to a suitable finite differential equation results in

$$\begin{aligned} & (\theta_{m+1,n} - 2\theta_{m,n} + \theta_{m-1,n}) + \left( \frac{k_{m+1,n}}{k_{m,n}} - 1 \right) \\ & \times (\theta_{m+1,n} - \theta_{m,n}) = \frac{1}{\alpha_{m,n}} \frac{(\Delta x)^2}{\Delta t} (\theta_{m,n+1} - \theta_{m,n}) \quad (4) \end{aligned}$$

where the coordinates of a typical grid point are  $x = m\Delta x$  and  $t = n\Delta t$ , with  $m$  and  $n$  integers. If the effect of the conductivity term in Eq. (4) is neglected,

the error introduced in the determination of the thermal diffusivity is nevertheless low [14]. From Eq. (4) thermal diffusivity can be estimated as

$$\alpha_{m,n} = \frac{(\Delta x)^2}{\Delta t} \left[ \frac{\theta_{m,n+1} - \theta_{m,n}}{\theta_{m+1,n} - 2\theta_{m,n} + \theta_{m-1,n}} \right] \quad (5)$$

This result implies that if the time dependence of the temperature at three equally spaced points is known, the thermal diffusivity of the sample at the central point will be determined.

### 3. Experimental

#### 3.1. Sample preparation

The rubber compounds used in this work were prepared with natural rubber (NR, SMR20) and styrene-butadiene rubber (SBR–1502). The molecular weights of the polymers were measured by GPC and values of  $M_n = 91,350$  g/mol and  $M_n = 146,900$  g/mol were obtained for SBR and NR, respectively. The polydispersity indexes were  $PDI(NR) = 8.2$  and  $PDI(SBR) = 3.6$ . The densities of the polymers at room temperature are  $\rho(NR) = 0.917$  g/cm<sup>3</sup>,  $\rho(SBR) = 0.935$  g/cm<sup>3</sup>.

Seven samples were prepared with the compound formulations given in Table 1. These blends were mixed in a laboratory mill. First, a master batch with the two elastomers was prepared and then the curatives were added to complete the mixing. The blends were characterized at 433 K by means of torque curves in an Alpha MDR 2000 rheometer that are plotted in Fig. 1. In the case of the compound with 100% NR (sample A), the curve is shown including the reversion zone. From these curves the time to achieve the maximum torque,  $t_{100}$ , was obtained for each sample. These values are also given in Table 1.

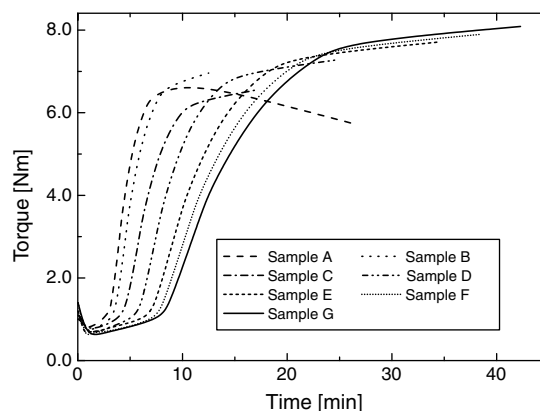


Fig. 1. Rheometer torque curves at 433 K as a function of the cure time for all the samples analyzed. In sample A, the reversion zone is included in the plot.

Samples in the form of sheets of  $150 \times 150 \times 2$  mm were cured in a mould at 433 K in a press up to time  $t_{100}$ . The applied pressure was 8.9 MPa. The samples were cooled rapidly in ice and water at the end of the curing cycle. The density  $\rho$  of each cured compound was measured and is given in Table 1.

#### 3.2. Diffusivity measurements

Our device is based on a continuous heating method that was used by Hands and Horsfall [15] for measuring the thermal diffusivity of rubber compounds. In the last years we have improved this type of technique, and substantial research work has been performed in the process [7–10].

Fig. 2 shows a schematic drawing of the device developed to measure changes in temperature inside the sample produced by heating both surfaces of the sample.

Table 1  
Compound formulations (in phr), density,  $t_{100}$  (MDR2000, 433 K)

Materials	A	B	C	D	E	F	G
SBR1502	–	10	25	50	75	90	100
NR- SMR20	100	90	75	50	25	10	–
Stearic Acid				2			
ZnO				5			
Antioxidant				1.2			
Sulfur				2.25			
TBBS				0.7			
$t_{100}$ (min)	10.7	12.8	17.0	24.7	34.4	38.5	42.3
$\rho$ (g/cm <sup>3</sup> )	0.954	0.958	0.957	0.965	0.972	0.973	0.979

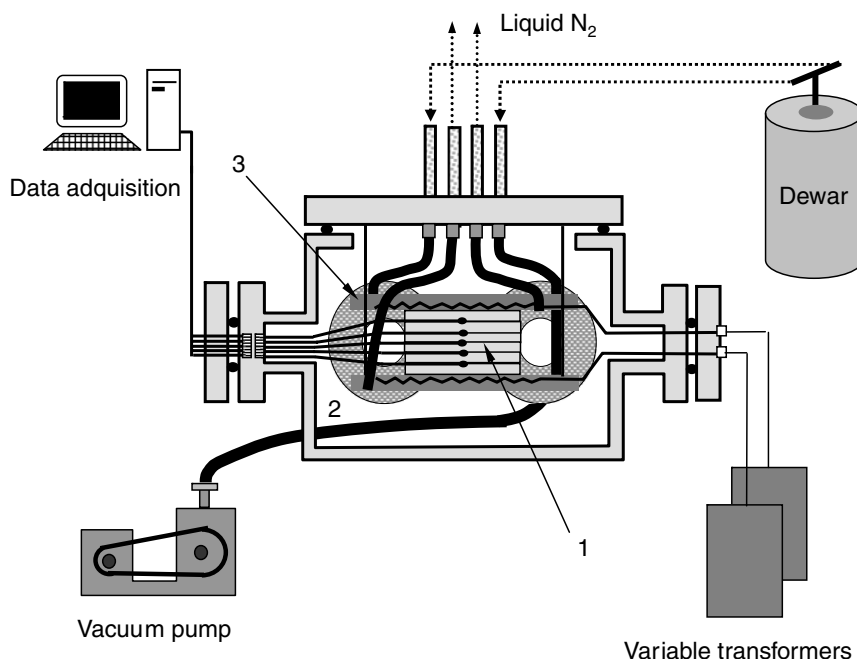


Fig. 2. Schematic drawing of thermal diffusivity device. Sample (1), vacuum chamber (2), heater platens (3).

Six sheets of equal thickness of the sample (1) that are sandwiched between two square brass plates (3) compose the measuring cell. Both brass platens have cylindrical internal channels, in which coolant fluid can circulate.

In mutual contact with these brass platens, there is an electrical plate heater, sheathed in stainless steel that provides physical strength and good thermal conductivity. These heaters can be heated at a controlled rate.

The aspect ratio of the assembled sample is about 1:10 so that the heat flow through the thickness at the center of the measuring cell can be considered one-dimensional.

As it can be observed in Fig. 2, the cell (1) is placed in a vacuum chamber of cylindrical shape (2) made of stainless steel in order to avoid condensation when the test is performed below room temperature, or oxidation if the it is performed a higher temperatures. The chamber is sealed with a stainless steel top plate. This plate allows the introduction of four pipes connected to four flexible tubes and through which liquid nitrogen is passed to the top and bottom platens of the measuring cell.

The samples to be analyzed are cut in six square-shaped pieces. The samples were sheets of 80 mm × 80 mm and 2 mm of thickness.

The change of temperature in the cell is measured by means of five iron-constantan (J) thermocouple wires of 0.2 mm diameter. This thickness was chosen to eliminate sources of error in the measurements due to conduction of heat along the thermocouple wires. The five thermocouple wires were arranged so that their junctions lie as closely as possible to the axis of symmetry of the device. The positions of the thermocouple wires are shown in Fig. 3.

Thermocouple data were taken by a PC with a Keithley DAS8/PGA 12 bit A/D conversion board. Acquisition data software was developed in Turbo C and allows obtaining 800 reading/s for each of the five channels used in the experiment.

The following method was used: if  $n$  temperature measurements were registered in a time interval  $\Delta t$ , a central value is taken in this interval, and to determine the temperatures corresponding to this value, the following least square fit was used

$$E_j^2 = \sum_{i=1}^n (f(t_i) - \theta_i)^2 \quad (6)$$

where  $\theta_i$  is the recorded temperature at time  $t_i$  and  $f$  is the fit function which was chosen as a second order polynomial in time.

Once the cell is placed in the chamber and the latter is closed, vacuum is made using a vacuum pump

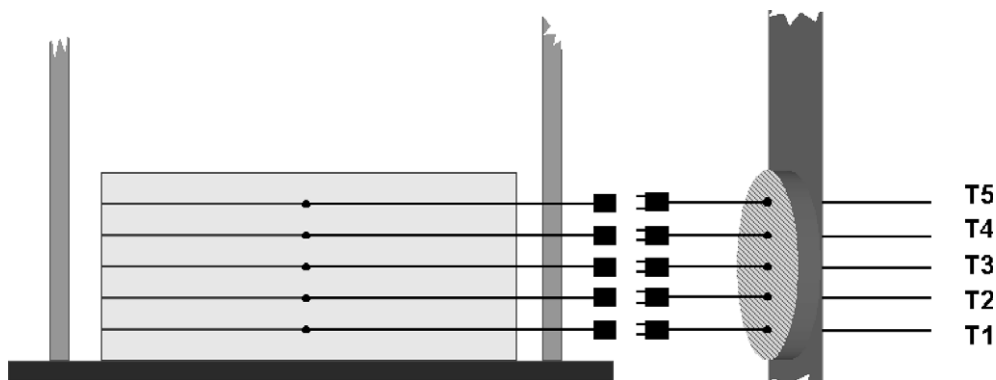


Fig. 3. Position of the thermocouple wires in the measuring cell. Each thermocouple wire,  $T_1$  to  $T_5$ , is placed between two cured sheets of the sample to be measure.

until a pressure of 1.3 Pa is reached. Then the cell is cooled with liquid  $N_2$  pumped through the two inlet pipes (one for the upper plate and the other for the lower plate) until the temperature in the middle of the sample reaches a value close to 100 K.

The heating rate of the cell is regulated by means of two variable transformers that are used to supply the same electrical current to both heaters. In our experiments we use a heating rate of 9 K/min.

Cured samples of the prepared blends were measured in the range between 130 K and 400 K. Two heating scans were performed and the second one is reported.

### 3.3. DSC measurements

Thermal measurements of each cured sample were performed with a Mettler-Toledo 822 instrument, indium and zinc calibrated for temperature, heat flow and tau lag. Samples of about 7 mg were heated under a nitrogen atmosphere from 173 to 298 K, at a scanning rate of 9 K/min; sample mass was determined by means of a Sartorius balance with an accuracy of 0.01 mg. The glass transition temperature was evaluated as the inflection point of the heat flow curve versus temperature. Each thermogram was corrected for the asymmetry between the sample and the reference side in the DSC instrument by the subtraction of a blank curve, i.e. a heat flow curve detected with empty crucibles, that were the same used in the sample measurement, and were subjected to the same temperature time profile. After this correction, specific heat capacity curve as a function of temperature was directly obtained from the heat flow curve divided by the heating rate and the sample mass. For each sample, the thermogram of the sec-

ond heating run was adopted; care was taken in testing the reproducibility of the blank curves.

## 4. Results and discussion

Fig. 4 shows the  $T_g$  values for the cured NR/SBR blends obtained from the DSC scans. It is interesting to notice that in some of the samples two glass transition temperatures were detected ( $T_{g1}$  and  $T_{g2}$ ), in good agreement with internal friction results reported by Ghilarducci et al. [16] who studied similar cured blends. The presence of two  $T_g$  is one of the distinctive features of partial immiscible blends and each one of the  $T_g$  values is associated with the corresponding phases of the blend, i.e. NR and SBR.

Hourston and Song [17], based on results using modulated-temperature DSC, proposed that the amount of interface plays an important role in the heat capacity values of immiscible and partially

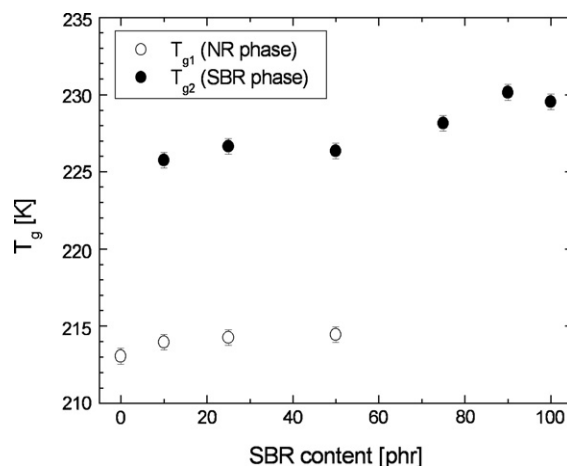


Fig. 4. Glass transition temperature,  $T_g$ , as function of the SBR content in the cured samples.

miscible rubber blends. They measured an uncured 50:50 NR/SBR blend and detected an increase in the value of  $dc_p/dT$  in the temperature region between the glass transitions of the two polymer phases. They also detected a decrease in the value of  $\Delta c_p$  at the glass transition temperatures of both polymers. According to these authors, these facts indicate the presence of an interfacial layer between components.

Upon analysis of our results, the blends containing 10 phr and 25 phr of NR only show one  $T_g$ . This fact must be carefully considered because there would be a dilution effect. The shift of the glass transition temperatures associated with each phase in the blend can be explained considering what happens with the network structure of each phase:

- (1) We should consider that the distribution of chemicals in each phase of the blend is the same as when the samples are prepared. Following the works of Mallon and McGill in IR/SBR blends [18–20], we think that there is a difference in reactivity of the two elastomers, NR and SBR towards TBBS/sulfur. At vulcanization temperatures, the solubility of both sulfur and accelerator is different in both elastomeric phases. However, NR initially crosslinks more rapidly than SBR, as can be observed in the rheometer curves given in Fig. 1. This fact implies that there is a rapid depletion of curatives in the NR phase of the blend and a replenishment of curatives due to the diffusion from the SBR phase. The consequence of these mechanisms is a zone of high crosslink density in the NR phase close to the interface, higher than in the case of pure NR compound. As it is known, the glass transition temperature increases as the crosslink density increase due to free volume effects [21].

At the same time, the migration of curatives from SBR to NR produces a fall in the crosslink density of the SBR phase when compared with the case of the pure SBR compound. Therefore, a lower value of the  $T_g$  is expected associated with the SBR phase.

- (2) When the blend gets richer in NR, a shift of the  $T_{g2}$  value (associated with the phase SBR) is observed toward lower values of temperature. Regarding the times of cure  $t_{100}$  of each blend in Table 1, it should be noticed that they diminish at higher NR content in the blend. This fact implies that the SBR phase

should be subcured in all the samples except in sample G (SBR100 phr) and thus the crosslink density will be lower in this phase compared with sample G.

The remaining fact to be considered is the migration of curatives towards the NR phase, which produces a drop in the crosslink density in the SBR phase as well. It is known that lower crosslink density implies lower glass transition temperatures [21].

- (3) When the blend gets richer in SBR, the  $T_{g1}$  value (associated with the NR phase) shifts to a slightly higher value compared with the glass transition temperature of the compound NR100 phr (sample A). In these compounds, the cure time  $t_{100}$  is higher than in sample A, which implies that the NR phase is overcured.

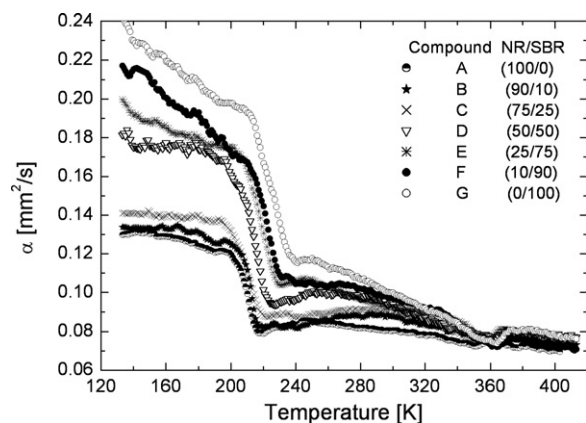


Fig. 5. Variation of the thermal diffusivity,  $\alpha$ , with temperature for all the cured blends analyzed.

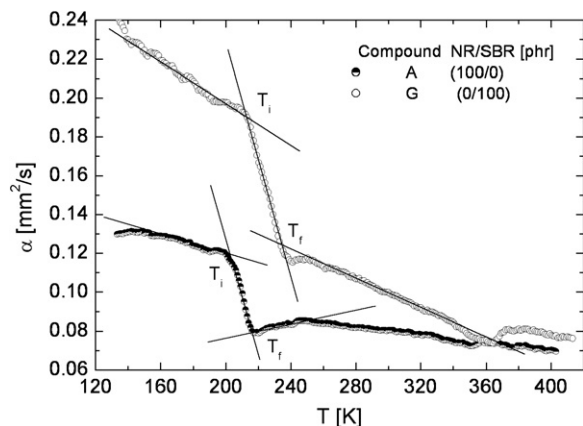


Fig. 6. Variation of the thermal diffusivity of vulcanized NR, SBR with temperature. The intersection of the regression lines limits the transition zone between the rubbery and glassy behavior.

Table 2

Glass transition temperatures,  $T_g$ , obtained from thermal diffusivity diagrams

Sample	$T_i$ (K)	$T_f$ (K)	$(T_f - T_i)$ (K)	$T_g$ (K)
A	204 ± 1	216 ± 1	12	210.0
B	207 ± 1	216 ± 1	9	211.5
C	199 ± 1	219 ± 1	20	209.0
D	201 ± 1	224 ± 1	23	212.5
E	207 ± 1	229 ± 1	22	218.0
F	214 ± 1	230 ± 1	16	222.0
G	214 ± 1	235 ± 1	21	224.5

$T_i$  = initial temperature of the glass transition zone.  $T_f$  = final temperature of the glass transition zone.

If it is considered that a constant level of curatives is present in the NR phase, it would be expected that there would be a decrease in the total crosslink density of NR phase. It is also expected that a change in the type of crosslinks in the network would occur with a higher density of monosulphides linkages and a corresponding loss of polysulphide link-

ages [22]. However, the presence of intramolecular incorporation of sulfur by cyclic structures or pendant sulphides would produce a considerable hindrance of chain mobility, which would be the cause of the shift of  $T_{g1}$  value at higher temperatures. Despite this, as it was mentioned previously, the migration of curatives from the SBR phase towards the NR phase would produce a local increase of the crosslink density in the NR interface and this fact would reduce the chain mobility in this zone with the consequence of an increase in  $T_{g1}$ .

Fig. 5 shows the plots of the thermal diffusivity as a function of temperature for all the compounds used in this study. The error in the diffusivity measurements was 3%. It can be seen that there is an abrupt change in the curves for each of the blends in the temperature range where the glass transition is expected to appear.

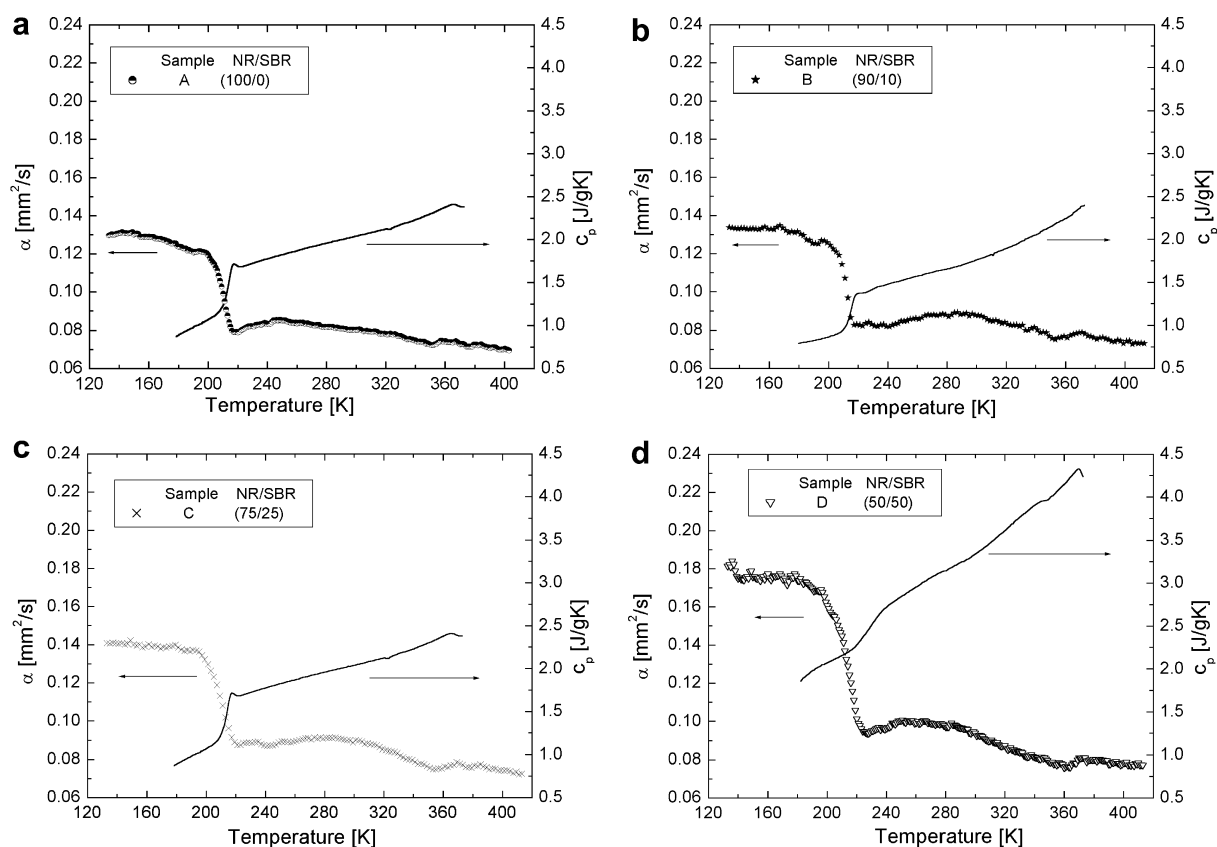


Fig. 7. Comparison between the variation of the thermal diffusivity,  $\alpha$ , and specific heat capacity,  $c_p$ , with test temperature for each cured blend. (a) Sample A (100 phr NR). (b) Sample B (90 phr NR/10 phr SBR). (c) Sample C (75 phr NR/25 phr SBR). (d) Sample D (50 phr NR/50 phr SBR). (e) Sample E (25 phr NR/75 phr SBR). (f) Sample F (10 phr NR/90 phr SBR). (g) Sample F (100 phr SBR).

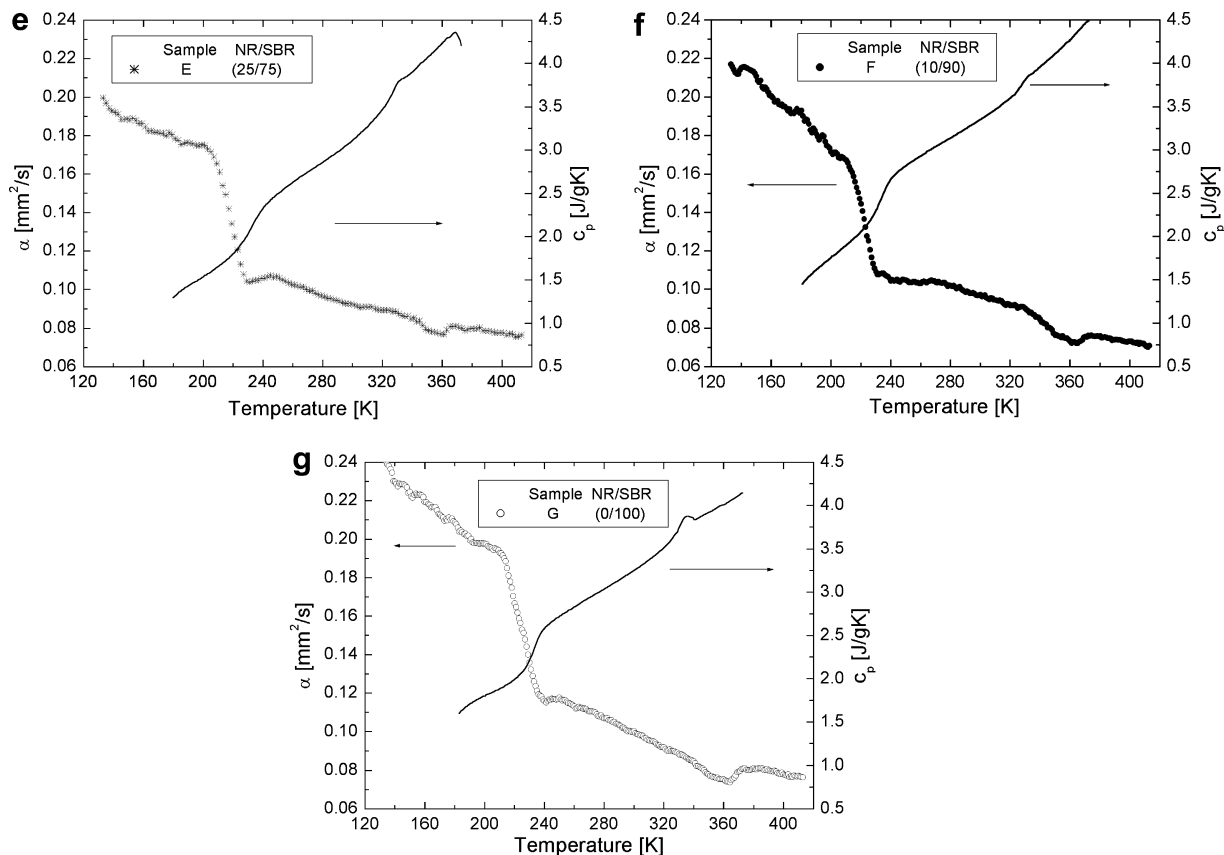


Fig. 7 (continued)

Fig. 6 shows the details of the glass transition region for each of the pure elastomers (samples A and G). To interpret this kind of diagram, three regression lines are drawn to each curve in the range of temperatures where the glass transition is expected. Three temperatures can also be defined:  $T_i$ ,  $T_f$  and  $T_g$ . The temperature  $T_i$  corresponds with the intersection point of the regression line of the glassy zone and the transition zone. On the other hand, the temperature  $T_f$  is that of the intersection of the regression line of the transition and rubbery zones. Finally, the value of  $T_g$  corresponds in this analysis to the middle point  $(T_i + T_f)/2$ . These values are given in Table 2 for all the measured samples. In the case of the diffusivity measurements it was not possible to distinguish two glass transition temperatures in the blends as in the case of the DSC analysis.

Fig. 7 shows a plot of both diffusivity and the specific heat capacity for each of the samples analyzed. These figures show that both physical entities detect the transition zone of the compounds.

The range of variation of  $c_p$  is similar in samples A, B and C, while the range  $c_p$  increases and is shifted towards higher values from samples D to F, with increasing SBR content. This is in accordance with the trend of  $c_p$  for NR and SBR separately. Moreover,  $c_p$  for an immiscible polymer blend is a weighted mean of the  $c_p$  value of the constituents; the presence of an interface causes an increase in the heat capacity [17].

The distribution of the phases, geometry and orientation of the dispersed phase influences the thermal conductivity and diffusivity of heterogeneous media as elastomer blends. Considering the volume fractions (or the weight fractions) and the thermal diffusivities of the two-phases, it is possible to establish the upper and lower bound of the thermal diffusivity of the blend.

If the two-phases are arranged parallel to the direction of the heat flow the blend thermal conductivity (and also thermal diffusivity) can be expressed following a mixture law. On the other hand, if the two-phases are arranged perpendicular to the direc-



tion of the heat flow, the thermal diffusivity is given by series conduction through both phases [23].

In Fig. 5, it is interesting to analyze what happens in the transition zone of the studied blends. With decreasing temperatures, the SBR phase undergoes a glass transition while the NR phase remains in the rubbery state. Fig. 8 shows the values of the thermal diffusivity at 220 K, a temperature where this behavior is observed. These values have an excellent correlation with the following relationship

$$\frac{1}{\alpha_c} = \frac{\omega_{\text{NR}}}{\alpha_{\text{NR}}} + \frac{\omega_{\text{SBR}}}{\alpha_{\text{SBR}}} \quad (7)$$

with a regression coefficient  $R^2 = 0.995$ . This equation is a representation of a serial thermal conduction where  $\omega_{\text{NR}}$  and  $\omega_{\text{SBR}}$  are the weight fractions of NR and SBR in the blend and  $\alpha_{\text{NR}}$  and  $\alpha_{\text{SBR}}$  are the thermal diffusivities of the pure cured elastomers.

We also use Eq. (7) to fit the thermal diffusivity of the samples in the rubbery and in the glassy zones. We chose two representative temperatures: 180 K for the glassy zone and 300 K for the rubbery zone. In the glassy zone, the fit is good with a regression constant  $R^2 = 0.951$ . In the other hand, in the rubbery zone, the fit of Eq. (7) to the experimental data is not as good as in the transition zone, with  $R^2 = 0.889$ . The lines plotted in Fig. 8 are the lines given by Eq. (7).

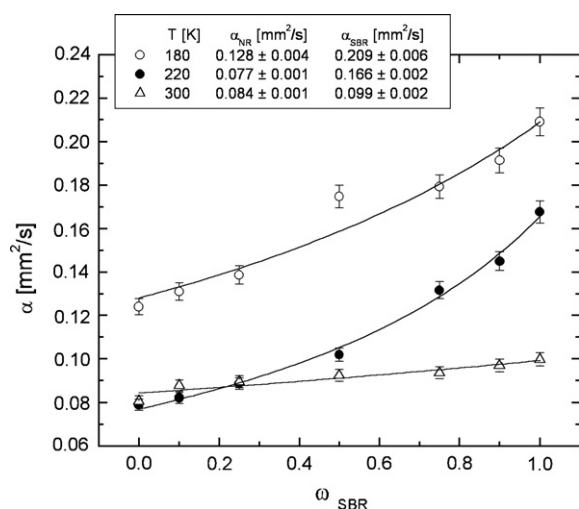


Fig. 8. Variation of the thermal diffusivity with the weight fraction of SBR in the blend, at three temperatures: glassy zone (180 K), transition zone (220 K) and rubbery zone (300 K). The line is the fit of the experimental data to Eq. (7). The obtained parameters of Eq. (7),  $\alpha_{\text{NR}}$  and  $\alpha_{\text{SBR}}$  are also given.

We notice that in the rubbery region (curve at 300 K in Fig. 8) the deviation between the experimental values and Eq. (7) is higher for the cured NR sample. It can be thought that the presence of the local increase of the crosslink density in the NR interface would have some influence in this case. However, further study is required to elucidate this point.

## 5. Conclusions

Our present work leads to the following conclusions:

In NR/SBR blends prepared with TBBS(accelerator)/sulfur and vulcanized at 433 K, there is not a unique glass transition temperature measured with DSC. Two glass transitions are obtained, each one corresponding to each phase of the blend. These temperatures are not the same in all the blends and depend on the crosslink density in each polymer phase and the interface.

The thermal diffusivity was measured in the NR/SBR cured blends and its variation with temperature shows clearly the transition zone. However, it was not possible to distinguish the  $T_g$  of each phase. Instead an apparent single  $T_g$  is observed for each blend.

A serial thermal conduction, model considering the weight fraction of each elastomer and their thermal diffusivity, can be used to explain the thermal diffusivity of the blend in the transition and glassy zones. In the case of the rubbery zone, the model should be improved in order to obtain a better fit.

## Acknowledgments

This work was supported by the Universidad de Buenos Aires, Argentina (Investigation Project X191 and X808), Consejo Nacional de Investigaciones Científicas y Tecnológicas (Argentina) and Agencia Nacional de Investigaciones Científicas y Tecnológicas (Argentina).

The authors want to thank Fate SAICI (Argentina) for the preparation of the samples.

## References

- [1] Sheindlin M, Halton D, Musella M, Ronchi C. Advances in the use of laser-flash techniques for thermal diffusivity measurement. *Rev Sci Instrum* 1998;69:1426–36.
- [2] Banaszkievicz M, Seiferlin K, Spohn T, Kargl G, Komle N. A new method for the determination of thermal conductivity

- and thermal diffusivity from linear heat source measurements. *Rev Sci Instrum* 1997;68:4184–90.
- [3] Murashov VV, White MA. Apparatus for dynamical thermal measurements of low-thermal diffusivity particulate materials at subambient temperatures. *Rev Sci Instrum* 1998;69:4198–204.
- [4] Pourpoint TL, Banish RM, Wessling FC, Sekerka RF. Real-time determination of thermal diffusivity in a disk-shaped sample: applications to graphite and boron nitride. *Rev Sci Instrum* 2000;71:4512–20.
- [5] Vozár L, Groboth G. Thermal diffusivity measurement of poorly conductive materials: a comparison of step-heating and flash methods. *High Temp–High Press* 1997;29:191–9.
- [6] Kubičár L, Boháč V. A step-wise method for measuring thermophysical parameters of materials. *Meas Sci Technol* 2000;11:252–8.
- [7] Mariani MC, Beccar Varela MP, Marzocca AJ. An improvement in the determination of thermal properties of elastomeric compounds. *Kautsch Gummi Kunstst* 1997;50:39–42.
- [8] Camaño E, Martire N, Goyanes SN, Marzocca AJ, Rubiolo GH. Evaluation of thermal diffusivity of rubber compounds through the glass transition range. *J Appl Polym Sci* 1997;63:157–62.
- [9] Goyanes SN, Beccar Varela MP, Mariani MC, Marzocca AJ. Influence of the carbon black dispersion in the thermal diffusivity of a SBR vulcanizate. *J Appl Polym Sci* 1999;72:1379–85.
- [10] Goyanes SN, Marconi JD, König PG, Rubiolo GH, Matteo CL, Marzocca AJ. Analysis of thermal diffusivity in aluminum (particle) filled PMMA compounds. *Polymer* 2002;42:5267–74.
- [11] Vilgis TA, Heinrich G. Crosslinked polymer blends: theoretical problems from rubber physics to technology. *Kautsch Gummi Kunstst* 1995;48:323–35.
- [12] Sircar AK. In: Turi EA, editor. *Thermal characterization of polymeric materials*. San Diego: Academic Press; 1981. p. 887–1378.
- [13] Saxena NS, Pradeep P, Mathew G, Thomas S, Gustafsson M, Gustafsson SE. Thermal conductivity of styrene butadiene rubber compounds with natural rubber prophylactics waste as filler. *Eur Polym J* 1999;35:1687–93.
- [14] Beccar Varela MP, Mariani MC, Marzocca AJ, Rial DF. Estimation of the dependence of the elastomer thermal diffusivity with the temperature. In: D'Attellis CE, Fernandez-Berdaguer EM, editors. *Proceeding of the first latin American workshop of applied mathematicae in industry and medicine*. Buenos Aires: CLAMI; 1996. p. 183–6.
- [15] Hands D, Horsfall F. The thermal diffusivity and conductivity of natural rubber compounds. *Rubber Chem Technol* 1977;50:253–65.
- [16] Ghilarducci A, Cervený S, Salva H, Matteo CL, Marzocca AJ. Influence of the blend composition the internal friction of NR/SBR compounds. *Kautsch Gummi Kunstst* 2001;54:382–6.
- [17] Hourston DJ, Song M. Quantitative characterization of interfaces in rubber–rubber blends by means of modulated-temperature DSC. *J Appl Polym Sci* 2000;76:1791–8.
- [18] Mallon PE, McGill WJ. Polyisoprene, poly(styrene-cobutadiene), and their blends. I Vulcanization reactions with tetramethylthiuram disulfide/sulfur. *J Appl Polym Sci* 1999;74:1250–63.
- [19] Mallon PE, McGill WJ. Polyisoprene, poly(styrene-cobutadiene), and their blends. Part II. Vulcanization reactions with 2-bisbenzothiazole-2,2' disulfide/sulfur. *J Appl Polym Sci* 1999;74:1264–70.
- [20] Mallon PE, McGill WJ. Polyisoprene, poly(styrene-cobutadiene) and their blends. III. Tensile properties of tetramethylthiuram disulfide/sulfur and 2-bisbenzothiazole-2,2'-disulfide/sulfur compounds. *J Appl Polym Sci* 1999;74:2143–9.
- [21] Shefer A, Gottlieb M. Effect of cross-link on the glass transition temperature of end-linked elastomers. *Macromolecules* 1992;25:4036–42.
- [22] Marzocca AJ, Steren CA, Raimondo RB, Cervený S. Influence of the cure level on the monomeric friction coefficient of natural rubber vulcanizates. *Polym Int* 2004;56:646–55.
- [23] Gehman SD. Heat transfer in processing and use of rubber. *Rubber Chem Technol* 1967;40:36–99.